Research Article

Suleiman MJ. Enjadat*

CFD Comparison of multiphase models in the pool boiling state

https://doi.org/10.1515/cls-2022-0029
Received Dec 22, 2021; accepted Apr 01, 2022

Abstract: With the development of simulation technology and programs, it became necessary to study the models that control equations' solutions and influence the results. The models having control over solving equations of multiple phases and materials are investigated. They include (Volume of Fluid (VOF), mixture, Eulerian) controlling the governing equations. The study was conducted depending on the boiling point of the water. The activation of these three models is carried out to find out which one is better for solving the issue of boiling compared to previous numerical and empirical research with the study of the surface tension coefficient that affects the behavior of phases in a contaminated manner. The best model explored in the case of boiling is VOF for the merging of steam bubbles, the velocity of flows 0.257 m/s for both water and steam, and the phase transition. The effectiveness of the VOF model is mirrored by higher efficiency and accuracy of the solution with velocity 0.257 m/s and volume fraction 0.9997. The activation of the surface tension factor 0.072 property simulates the real conditions surrounding the materials used in boiling, but it significantly increases the turbulence and distribution of gas bubbles.

Keywords: Nucleate pool boiling, VOF model, mixture model, Eulerian model

1 Introduction

The Volume of Fluid (VOF) and the Surface of Fluid (SAOF) are being used to model the two-phase upward flow. Eulerian models. The mathematical formulations of these models cause differences in convergence, computing time, and accuracy. The VOF model only anticipates the pattern movement. This research modeled six tests on an orthogonal (butterfly) grid [1]. When the bulk fluid temperature is lower than the saturation temperature, and the fluid temperature approaches the saturation near the tube wall, the subcooled boiling heat transfer regime occurs in a heated vertical channel. This discovery will greatly aid thermal-hydraulic analyses of pressurized water reactors. Compared to the experimental data, the estimated wall temperature at the fluid border is rather consistent [2]. This paper demonstrates the creation and verification of a kernel boiling model in the OpenFOAM Fluid Volume Analyzer. Both natural contact evaporation, which is often not resolved by the digital network, and conjugate heat exchange between solid and liquid are distinguished. The adsorption interface problem using validation simulation and spherical bubbles' generation succeeded [3]. This research focuses on the numerical representation of bubble development and the underlying interface deformation problem related to phase shift in VOF interface tracking. It presents a cell alternation algorithm that distinguishes between two types of cells close to the interface [4]. Under boiling conditions in a pool, numerical analysis detects the quantitative impacts of essential elements on the detachment properties of disconnected air pockets. The effect of the introductory warm limit thickness (ITBL) on the bubbling of immersion lakes for R113, just as the effects of surface wettability, divider temperature, and level of gravity, were contemplated in the recreations [5]. For the two-stage stream and hotness move in a little channel, the reenactment results are contrasted and the tests. The low request model is utilized to show the mass exchange between stages. The outcomes show that the worth of the steady ought to fluctuate across the space using various choices [6]. The development of bubble off-gases results from the unavoidable loss of hotness from the environmental factors in the LNG tank, regardless of the broad protection. The prevailing bubbling cycle is surface dissipation, and center bubbling is phenomenal with satisfactory protection [7]. Due to the higher measure of hotness that can be conveyed, bubbling streams are normal in industry and design. Bubbling affects the activity of all water-cooled atomic reactors in the nuclear business. CFDs are created to address hardships with thermo-water driven wellbeing, such as deciding basic hotness stream [8]. The heater was explored in a shut two-stage convection broiler

***Corresponding Author: Suleiman MJ. Enjadat:** School of Engineering, Mechanical Engineering Department, The University of Jordan, Amman 11942 Jordan; Email: suliemanenjadat@gmail.com

utilizing a blend of CFD and representation. A normally used stage change model, Lee's model, is altered by joining superheat into the situation to further develop forecast execution [9]. Interestingly, CFD reproductions have anticipated the bubbling framework and the two-stage stream design with water at low energy yield, known as evaporator bubbling. The polyphase stream qualities of a non-fiendish hotness pipe have been effectively planned and envisioned utilizing reproductions [10]. A bubbling model is produced using the computational liquid elements (CFD) code to work out the source term for a coolant spill. The impact of worldwide temperature change on the pace of coolant dissipation is remembered for the model [11]. This paper talks about true cryogenic bubbling strategies utilizing computational liquid elements. The model inspects the cycles inside a warmed fuel gathering channel. Basic regions can be recognized by assessing the surface temperature of the pole, which can ultimately make the center bubble and harm the fuel pin [12]. In this paper, a CFD (Computational Fluid Dynamics) CFX model is utilized to reenact the hotness stream bubbling of refrigerant R-113 in an upward annular channel. By and large, there was great subjective concurrence with the test results [13]. We look at the current abilities of CFD for bubbling dividers in this paper. Bubbling water under high tension conditions, which is vital for thermal energy stations, was recently planned comparatively. It has been exhibited that different tests can be reenacted utilizing a solitary arrangement of model boundaries under a predefined scope of conditions [14]. The current capacities of CFD for bubbling dividers were inspected in this paper. The computational model utilized joins the parting of the hotness stream with a two-stage Euler/Euler stream depiction. Beforehand, fundamentally the same as models were used to reproduce bubbling water under states of high tension, which is basic for thermal energy stations [15]. The novelty of this work is translated by the requirements of effective numerical simulations to model and analyze the multiphase models in the pool boiling state of water, as few research publication and articles discussed this topic and make a comparison with several governing equations.

2 Methodology

The work was completely done by designing, simulating, and extracting the ANSYS CFD program results for analyzing and simulating fluids and refractories in general. The model was developed using two dimensions, a width of 10 cm, and a length of 8 cm, as a mini-model.

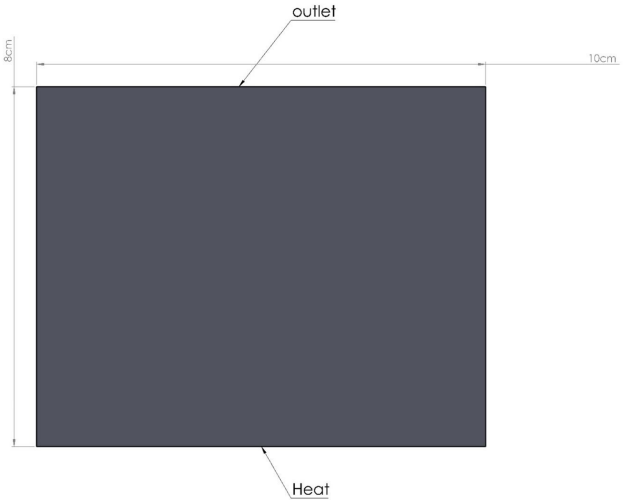

Figure 1: Geometry dimensions

Where the mesh was done accurately, the correct results were obtained during the simulation process, where the values of stability of speed appear with the number of elements, the logical picture of the sufficiency of the meshing process.

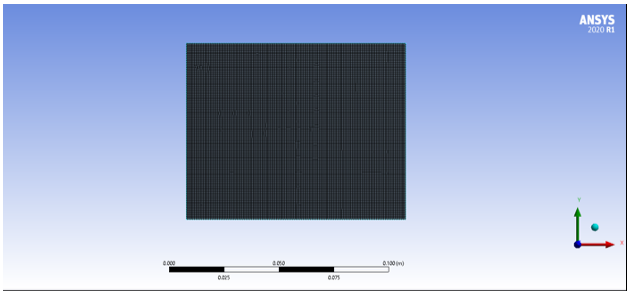

Figure 2: Geometry mesh

Table 1: Mesh depended

Case	Node	Element	Velocity (m/s)
1	6234	5347	0.3157
2	12800	12678	0.2589
3	32365	32004	0.2039
4	63243	61434	0.2041

The boiling process of water takes place at a temperature of 100°C, as the initial state of all simulated cases started at this temperature. The lower surface of the basin was subjected to a constant temperature of 110°C to continue the boiling state. The time step was 0.01 of a second,

and the number of steps was 500 for each case. The surface tension coefficient model was used for each scenario. It has a value of 0.072 to see the changes in the reactivity of the phase of the material.

3 Governing equations

The Eulerian concept is used to build ANSYS' wall boiling models. Polyphase flows are governed by phase continuity, momentum, and energy conservation laws. The boiling-wall phenomenon was modeled using Kurual and Podowski's RPI nucleate boiling model and Lavieville's extended-release nucleophilic (DNB) system formulation.

3.1 RPI model

The overall wall-to-fluid heat flow is divided into three components, according to the basic RPI model: convective heat flow, quenching heat flow, and evaporative heat flow:

$$\dot{q}_W = \dot{q}_C + \dot{q}_Q + \dot{q}_E \tag{1}$$

The hot wall surface is split into two categories: A_b (covered by nucleating bubbles) and $1 - A_b$ (covered by fluid).

- The convective heat flux $\dot{q}_C$ is denoted by

$$\dot{q}_C = h_C (T_w - T_1)(1 - A_b) \tag{2}$$

  T_w and T_l are the temperatures of the wall and the liquid, respectively. correspondingly, and h_c is the single-phase heat transfer coefficient.
- After bubble detachment, the quenching heat flux $\dot{q}_Q$ approximates the cyclic averaged transient energy transfer associated with liquid filling the wall area, and is given as

$$\dot{q}_Q = \frac{2k_l}{\sqrt{\pi\lambda_l T}} (T_w - T_l) \tag{3}$$

  Where k_l is the conductivity, T is the periodic fime, and $\lambda_l = \frac{k_l}{\rho_l t_{pl}}$ is the diffusivity.
- $\dot{q}_E$ denotes the evaporative flow.

$$\dot{q}_E = V_d N_w \rho_v h_{fv} \tag{4}$$

  Where V_d indicates the bubble volume dependent on the diameter of the bubble's departure, N_w indicates the density of active nucleate sites, ρ_v represents the vapor density, h_{fv} represents the latent heat of evaporation, and f represents the bubble departure frequency. The following parameters need closure in these equations:
- Field of impact
  Its definition focuses on the nucleate site density and the departing diameter [16]:

$$A_b = K \frac{N_w \pi D_W^2}{4} \tag{5}$$

Note that the area of influence must be limited to prevent numerical instability induced by unbound empirical correlations for the density of nucleate sites The list includes the regions of influence [16, 17]:

$$A_b = min\left(1, K \frac{N_w \pi D_w^2}{4}\right) \tag{6}$$

The empirical constant K is usually set to 4, although it has been revealed that this value is not universal and can range between 1.8 and 5. Based on the work of Del Valle and Kenning, the following relationship for this constant has been adopted [16, 17]:

$$K = 4.8e^{\left(-\frac{Ja_{ato}}{80}\right)} \tag{7}$$

and Ja_{sub} is defined as the subcooled Jacob number [16, 17]

$$Ja_{sub} = \frac{\rho_l C_{pl} \Delta T_{sub}}{\rho_v h_{fv}} \tag{8}$$

where $\Delta T_{sub} = T_{sat} - T_l$

The frequency of bubble departure is normally used in RPI modeling process as opposed to the one based on inertia-controlled development (not really applicable to subcooled boiling) can be expressed by [16]

$$f = \frac{1}{T} = \sqrt{\frac{4g(\rho_l - \rho_v)}{3\rho_l D_w}} \tag{9}$$

A relationship based on wall superheat is proposed. frequently used it to depict nucleate site density. The general expression of nucleation site density, N_w, can be expressed in the formula [16, 17]:

$$N_w = C^n (T_w - T_{sat})^n \tag{10}$$

Here, Lemmert and Chawla's empirical parameters are used, with n=1.805 and C=210. Other formulas, such as Kocamustafaogullari and Ishii, are also available, as illustrated in the formula [16]:

$$N_W^\star = f\left(\rho^\star\right) r_c^{\star -4.4} \tag{11}$$

$$N_w^\star = N_w D_w^2 \tag{12}$$

$$r_c^\star = \frac{2r_c}{D_w} \tag{13}$$

$$r_c = \frac{2\sigma T_{st}}{\rho_v h_f T T_w} \tag{14}$$

$$\rho^* = \frac{(\rho_1 - \rho_v)}{\rho_v} \tag{15}$$

The density function can be defined as D_w, where D_w is the bubble diameter and D_w is the density function [16]:

$$f\left(\rho^*\right) = 2.157 \times 10^{-7}\rho^{-4} \cdot 2\left(1 + 0.0049\rho^*\right)^{4.13} \tag{16}$$

The RPI model's default bubble departure diameter is calculated in meters and is based on empirical findings [16, 17]:

$$D_w = min\left(0.0014, 0.0006e - \frac{\Delta Tsub}{45.0}\right) \tag{17}$$

while Kocamustafaogullari and Ishii use [16]:

$$D_w = 0.0012\left(\rho^*\right)^{0.9} 0.0208\varnothing\sqrt{\frac{\sigma}{g\left(\rho_I - \rho_v\right)}} \tag{18}$$

In which the contact angle is determined in degrees.

Based on the Ünal relationship, the bubble departure diameter, D_w, in millimeters is calculated as [18, 19]:

$$D_w = 2.4210^{-5} p^{0.709}\left(\frac{a}{b\sqrt{\varphi}}\right) \tag{19}$$

$$a = \frac{\Delta T_{sup}}{2\rho_g H_{lv}}\sqrt{\frac{\rho_s C_{ps} k_S}{\pi}} \tag{20}$$

$$b = \begin{cases} \frac{\Delta T_{sub}}{2\left(1-\frac{\rho_\theta}{\rho_l}\right)} e^{\left(\frac{a\tau_{sk}}{3}-1\right)} & \Delta T_{sub} \le 3 \\ \frac{\Delta T_{sub}}{2\left(1-\frac{\rho_\theta}{\rho_r}\right)} & \Delta T_{sub} > 3 \end{cases} \tag{21}$$

$$\varphi = max\left(\left(\frac{U_b}{U_0}\right)^{0.47}, 1.0\right) \tag{22}$$

P is the flow pressure, $\Delta T_{sup} = T_w - T_{sat}$ is the wall superheat, H lv is latent heat, U_b is the near wall bulk velocity, and $U_b = 0.61$ m/s. The subscripts s, l, and g represent the solid, liquid, and vapor phases, respectively. Fluent's default model for bubble diameter as a function of local temperature is as follows sub cooling, $\Delta T_{sub} = T_{sat} - T_I$:

$$D_b = \begin{cases} max\left[1.0 \times 10^{-5}, \right. \\ \left. d_{min} \exp\left(\frac{-k(\Delta T_{m\omega} - \Delta T_{max})}{d_{min}}\right)\right] & \Delta T_{sub} > 13.5K \\ d_{max} - K\left(\Delta T_{sub} - \Delta T_{min}\right) & \Delta T_{sub} \le 13.5K \end{cases} \tag{23}$$

Where:

$$d_{min} = 0.00015m \tag{24}$$

$$d_{max} = 0.001m$$
$$\Delta T_{min} = 0K$$
$$\Delta T_{max} = 13.5K$$
$$K = \frac{d_{max} - d_{min}}{\Delta T_{max} - \Delta T_{min}}$$

As an alternative, the Ünal correlation may be used to get the bubble diameter, D_b [18]:

$$D_b = \begin{cases} 0.0015 & \Delta T_{sub} < 0 \\ 0.0015 - 0.0001\Delta T_{sub} & 0 \le \Delta T_{sub} \le 13.5K \\ 0.00015 & \Delta T_{sub} > 13.5K \end{cases} \tag{25}$$

The droplet diameter can be assumed to be constant or estimated to use the Kataoka-Ishii correlation when the flow regime switches to mist flow [20]:

$$D_d = C_{ds}\frac{\sigma}{\rho_v j_v^2} Re_l^{-1/6} Re_V^{2/3}\left(\frac{\rho_v}{\rho_l}\right)^{-1/3}\left(\frac{\mu_v}{\mu_l}\right)^{2/3} \tag{26}$$

Where: $C_{ds} = 0.28$

The vapor volumetric flow is denoted by j_v (superficial velocity). The local liquid is denoted by the symbol Re_l (the Reynolds number). The local vapor is denoted by Re_v. The Reynolds number, μ_l denotes the liquid viscosity, μ_v denotes the vapor viscosity.

As the bubbles leave the wall and go towards the subcooled area, heat transfer from the bubble to the liquid happens, which is referred to as

$$\dot{q}_{lt} = h_{sl}\left(T_{sat} - T_l\right) h_{sl} \tag{27}$$

h_{sl} is the volumetric heat transfer coefficient. The heat transfer coefficient may be calculated using the Ranz-Marshall or Tomiyama models presented in "The Heat Exchange Coefficient". The constant time scale return to saturation method is used to calculate the interface to vapor heat exchange. Rapid evaporation/condensation is intended to keep the vapor at the saturated temperature. The following formula [21]:

$$\dot{q}_{vt} = \frac{\alpha_v \rho_v C_{p,v}}{\delta t}\left(T_{sat} - T_v\right) \tag{28}$$

Where δt is the time scale set to a default value of 0.05 and $C_{p,v}$ is the isobaric heat capacity?

The evaporating mass flow is derived from the evaporation heat flux and supplied at the cell near the wall (Eq. (28)) [21]:

$$m_E = \frac{\dot{q}_E}{h_{fv} + C_{p,1}\Delta T_{sub}} \tag{29}$$

Interfacial mass transfer is wholly reliant on interfacial heat transfer. The interface mass transfer rate can be expressed as follows: Assuming that all heat transmitted

to the contact is utilised in mass transfer (evaporation or condensation), the interfacial mass transfer rate may be calculated as follows [21]:

$$m = \dot{m}_{lt} + \dot{m}_{vt} = \frac{\dot{q}_{lt} + \dot{q}_{vt}}{h_{fv}} \tag{30}$$

4 Results and discussions

Through this research paper, we can compare the computational models and know the best model for the boiling state of the liquid water in a basin, where through the results of the cases, we notice the difference in the distribution and flow of steam at the backward times.

Through the previous figures, we notice that the volume fraction of the vapor comes in a disordered form in the two models (a) and (b), while in the VOF model, we see the turbulence in the flow of steam upwards with the preservation of uniformity in the volume of the vapor space and with the progression of time we can confirm that the VOF model maintains the stability It boils and comes on smoothly.

We conclude that the flow velocity of the previous cases from the different models has variable values and shapes, as in the last figure. We note and confirm that the VOF model's flow speed comes more logically and closer to reality. And that each vapor bubble has its flowing speed, but in the rest of the models, we notice the high turbulence in the flow velocities.

The pressure values of the three models do not significantly impact the comparison process because we note the great convergence in the values and distribution concerning the pressures.

The value of the mass flow has a significant impact on the reliability and preference of the model, as it was found through the results that the value of the mass flow of the Eulerian model is 0.0751913 kg/s, the mixture is 0.0802918 kg/s, and VOF is 0.325981 kg/s where we note that the highest value of the mass flow is at the VOF model, which indicates the boiling in a complete and large.

The activation of the surface tension coefficient in the three models, with a real value of 0.072, leads to the cohesion of the water and steam atoms with the surrounding surfaces. Through the previous figure, we notice an increase

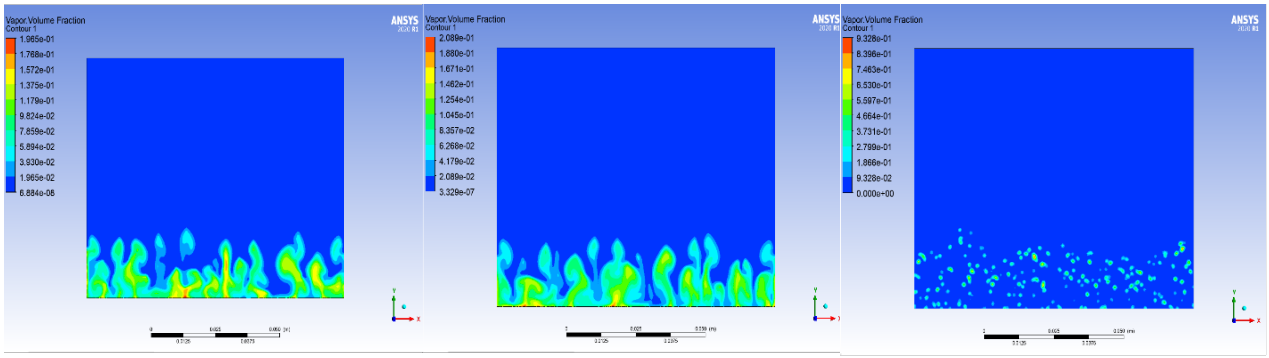

Figure 3: Volume fraction in 1 s. (a) Eulerian; (b) mixture; (c) VOF

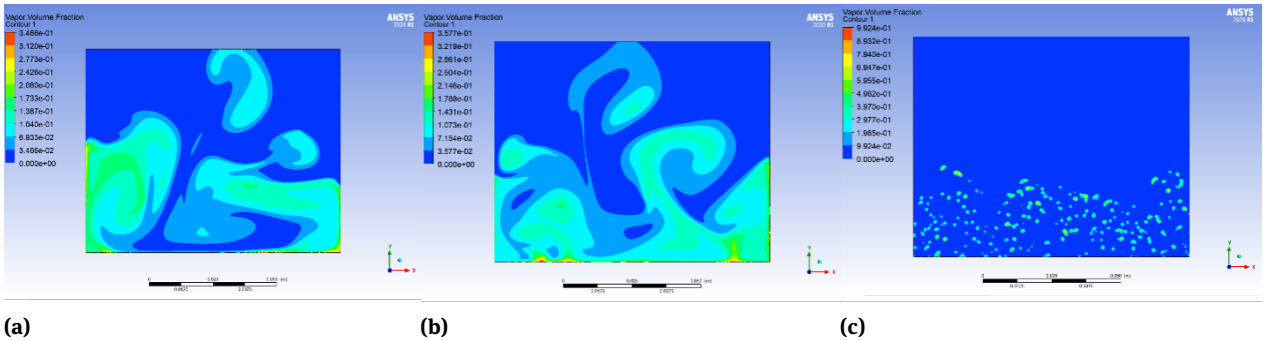

Figure 4: Volume fraction in 2 s. (a) Eulerian; (b) mixture; (c) VOF

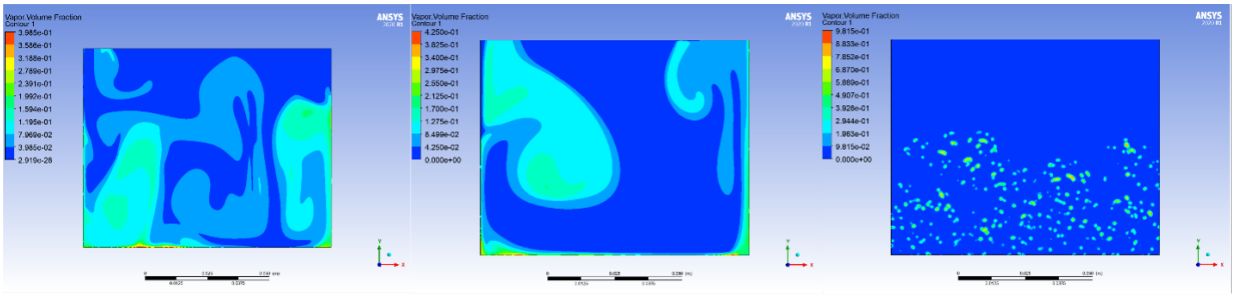

(a) (b) (c)

Figure 5: Volume fraction in 3 s. (a) Eulerian; (b) mixture; (c) VOF

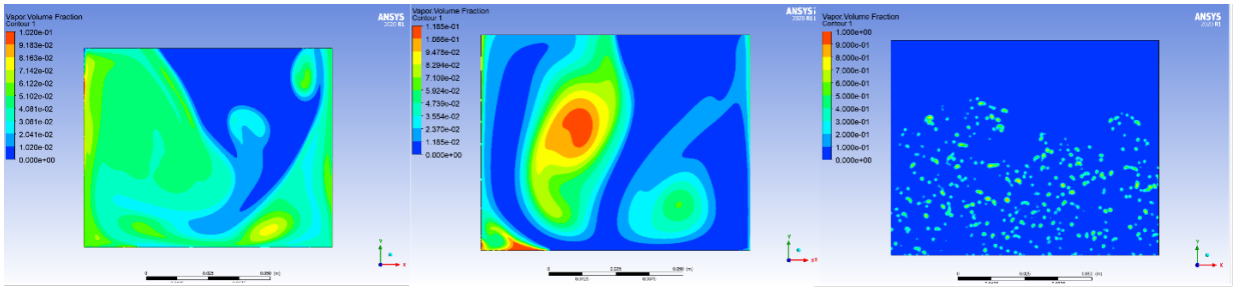

(a) (b) (c)

Figure 6: Volume fraction in 4 s. (a) Eulerian; (b) mixture; (c) VOF

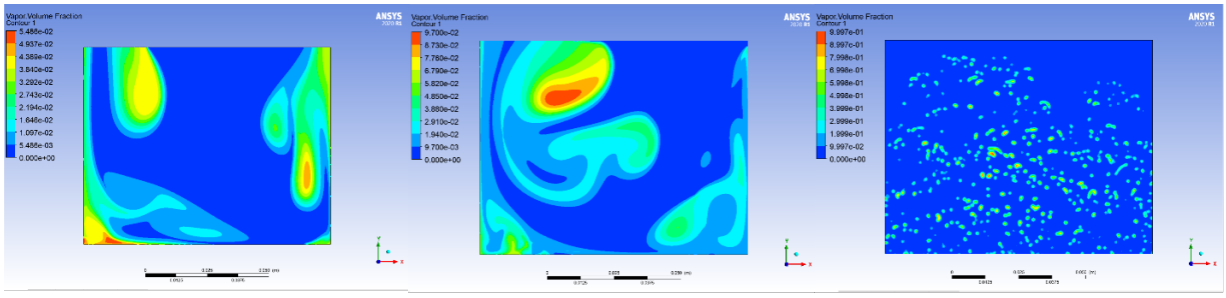

(a) (b) (c)

Figure 7: Volume fraction in 5 s. (a) Eulerian; (b) mixture; (c) VOF

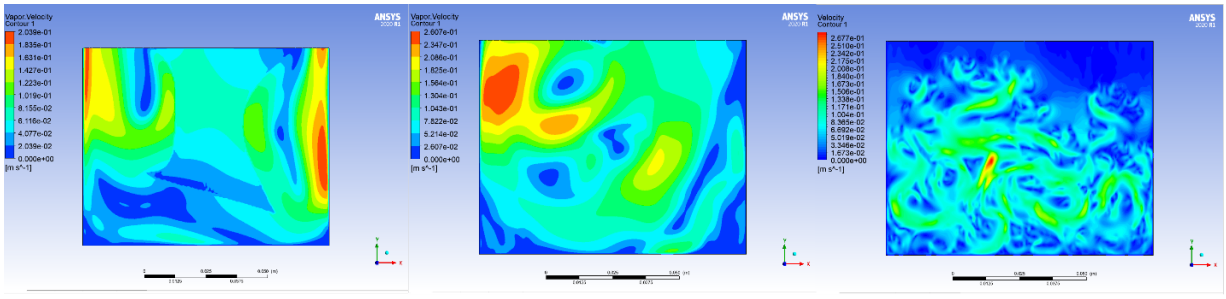

(a) (b) (c)

Figure 8: Velocity in 5 s. (a) Eulerian; (b) mixture; (c) VOF

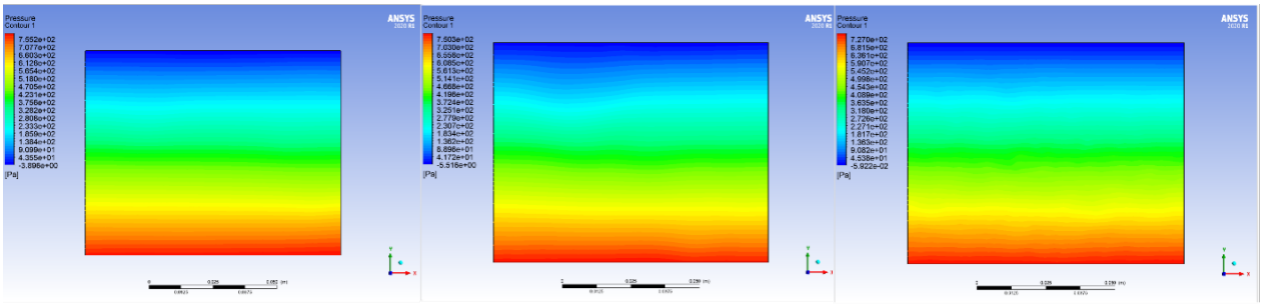

(a) (b) (c)

Figure 9: Pressure in 5 s. (a) Eulerian; (b) mixture; (c) VOF

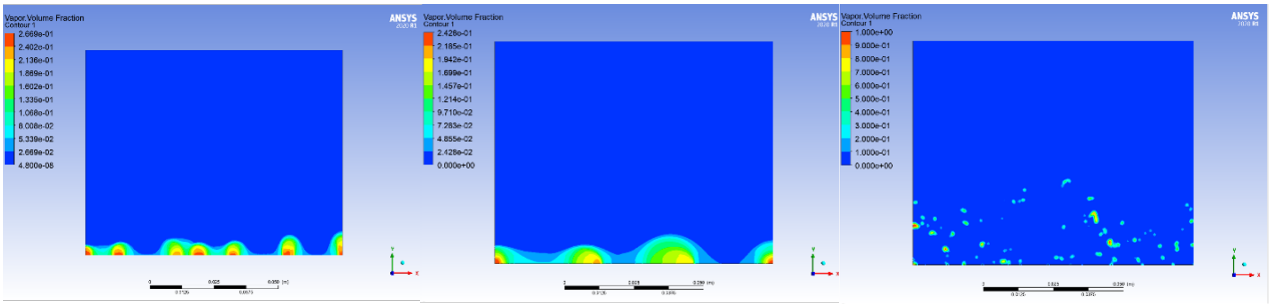

(a) (b) (c)

Figure 10: Volume fraction in 0.65 s. (a) Eulerian; (b) mixture; (c) VOF

in the largeness of steam bubbles in all the models that have been studied, which leads to an irregularity in the flow of steam bubbles outward, as it has less impact in the VOF model compared to the rest of the models and this is a positive thing for studying and understanding the models and choosing the best realistic model that can be worked with.

5 Conclusions

Studying and understanding models in engineering simulation programs help us choose the best model for each study or realistic engineering simulation. The three special models were verified in multiphase and with and without adding the surface tension coefficient. The major results of this work indicated that the best model studied in the case of boiling is VOF for the merging of steam bubbles, the velocity of flows 0.257 m/s for both water and steam, and the phase transition. In addition, findings revealed that the Eulerian model comes with accuracy in the second place after VOF for the convergence of its results. It is the most complex in solving equations as it details the velocities, flows, pressures. It is used to solve all the variables produced, preferably for each liquid or gas chosen compared to the other models. Where the velocity of the flow was 0.204 m/s is similar to the case of the VOF, which was 0.257 m/s. Furthermore, the findings confirmed that the model is a mixture, the values of the results are similar to the VOF model, but the distribution of gas bubbles and their diffusion is inaccurate and relatively unconsolidated. Also, the activation of the surface tension factor 0.072 property simulates the real conditions surrounding the materials used in boiling, but it increases the turbulence and distribution of steam bubbles significantly in all three models.

Funding information: The author states no funding involved.

Conflict of interest: The author states no conflict of interest.

References

[1] Georgoulas A, Andredaki M, Marengo M. An enhanced VOF method coupled with heat transfer and phase change to char-

acterise bubble detachment in saturated pool boiling. Energies. 2017 Mar;10(3):272.
[2] Braz Filho FA, Caldeira AD, Borges EM. Validation of a multidimensional computational fluid dynamics model for subcooled flow boiling analysis. 2011 International Nuclear Atlantic Conference – INAC 2011; 2011 Oct 24-28; Belo Horizonte, Brazil. ABEN; 2011.
[3] Kunkelmann C, Stephan P. CFD Simulation of Boiling Flows Using the Volume-of-Fluid Method within OpenFOAM. Numer Heat Transf A. 2009;56(8):631–46.
[4] Wang X, Wang Y, Chen H, Zhu Y. A combined CFD/visualization investigation of heat transfer behaviors during geyser boiling in two-phase closed thermosyphon. Int J Heat Mass Transf. 2018:121:703–714.
[5] Gorlé C, Lee H, Houshmand F, Asheghi M, Goodson K, Parida PR. Validation Study for VOF Simulations of Boiling in a Microchannel. Proceedings of the ASME 2015 International Technical Conference and Exhibition on Packaging and Integration of Electronic and Photonic Microsystems collocated with the ASME 2015 13th International Conference on Nanochannels, Microchannels, and Minichannels. Volume 3: Advanced Fabrication and Manufacturing; Emerging Technology Frontiers; Energy, Health and Water-Applications of Nano-, Micro- and Mini-Scale Devices; MEMS and NEMS; Technology Update Talks; Thermal Management Using Micro Channels, Jets, Sprays. 2015 Jul 6-9; San Francisco (CA), USA. ASME; 2015.
[6] Saleem A, Farooq S, Karimi IA, Banerjee R. A CFD simulation study of boiling mechanism and BOG generation in a full-scale LNG storage tank. Comput Chem Eng. 2018;115:112–20.
[7] Colombo M, Fairweather M. Accuracy of Eulerian–Eulerian, two-fluid CFD boiling models of subcooled boiling flows. Int J Heat Mass Transf. 2016;103:28–44.
[8] Borjini MN, Aissia HB, Halouani K, Zeghmati B. Effect of radiative heat transfer on the three-dimensional Boyancy flow in cubic enclosure heated from the side. Int J Heat Fluid Flow. 2008;29(1):107–18.
[9] Jouhara H, Fadhl B, Wrobel LC. Three-dimensional CFD simulation of geyser boiling in a two-phase closed thermosyphon. Int J Hydrogen Energy. 2016;41(37):16463–76.
[10] Liu Y, Olewski T, Véchot LN. Modeling of a cryogenic liquid pool boiling by CFD simulation. J Loss Prev Process Ind. 2015;35:125–34.
[11] Krepper E, Končar B, Egorov Y. CFD modelling of subcooled boiling – Concept, validation and application to fuel assembly design. Nucl Eng Des. 2007:237(7):716–731.
[12] Končar B, Krepper E. CFD simulation of convective flow boiling of refrigerant in a vertical annulus. Nucl Eng Des. 2008;238(3):693–706.
[13] Krepper E, Rzehak R. CFD for subcooled flow boiling: simulation of DEBORA experiments. Nucl Eng Des. 2011;241(9):3851–66.
[14] Krepper E, Rzehak R, Lifante C, Frank T. CFD for subcooled flow boiling: coupling wall boiling and population balance models. Nucl Eng Des. 2013;255:330–46.
[15] Kamel MS, Al-Agha MS, Lezsovits F, Mahian O. Simulation of pool boiling of nanofluids by using Eulerian multiphase model. J Therm Anal Calorim. 2020;142(1):493–505.
[16] Fincher SN. Numerical simulations of boiling in dielectric fluid immersion cooling scenarios of high power electronics [dissertation]. Auburn: Auburn University; 2014.
[17] Dong X, Zhang Z, Liu D, Tian Z, Chen G. Numerical investigation of the effect of grids and turbulence models on critical heat flux in a vertical pipe. Front Energy Res. 2018;6:58.
[18] Ünal HC. Maximum bubble diameter, maximum bubble-growth rate during the sub-cooled nucleate flow boiling of water up to 17.7 MN/m^2. Int J Heat Mass Transf. 1976;19:643–9.
[19] Michta E. Modeling of subcooled nucleate boiling with OpenFOAM [dissertation]. Stockholm: Royal Institute of Technology; 2011.
[20] Fore LB, Ibrahim BB, Beus SG. Visual measurements of droplet size in gas-liquid annular flow. Int J Multiph Flow. 2002;28(12):1895–910.
[21] Mao SF, Ji WT, Chong GH, Zhao CY, Zhang H, Tao WQ. Numerical investigation on the nucleate pool boiling heat transfer of R134a outside the plain tube. Numer Heat Transf A. 2019;76(11):889–908.